RSC Advances

PAPER

Cite this: *RSC Adv.*, 2016, **6**, 42572

Enhanced adsorption capacity of polypyrrole/TiO_2 composite modified by carboxylic acid with hydroxyl group†

Jiangtao Feng, Jie Chen, Ning Wang, Jingjing Li, Jinwen Shi* and Wei Yan*

Received 14th March 2016
Accepted 20th April 2016

DOI: 10.1039/c6ra06738g

www.rsc.org/advances

It was reported in our previous work that polypyrrole/TiO_2 (PPy/TiO_2) composite exhibited excellent adsorption ability for organic contaminants, and modification of the composite by different acids could greatly impact the adsorption performance. Herein, AC-PPy/TiO_2, SU-PPy/TiO_2, TA-PPy/TiO_2 and CI-PPy/TiO_2 composites were prepared in acetate (with only one carboxylic group), succinic (with two carboxylic groups), tartaric (with two hydroxyl and two carboxylic groups) and citric (with one hydroxyl and three carboxylic groups) acids, respectively. Acid Red G (ARG) as the typical anionic dye and Methylene Blue (MB) as the typical cationic dye were employed as the target removals to investigate the adsorption behavior of the as-prepared composites. It was found that the hydroxyl group in the employed carboxylic acids significantly affected the surface physicochemical properties and further the adsorption capacity of PPy/TiO_2 composite. TA-PPy/TiO_2 and CI-PPy/TiO_2 prepared in the carboxylic acids with hydroxyl group displayed enhanced adsorption capacity for either ARG or MB, which was 3–4 times higher than that of AC-PPy/TiO_2 and SU-PPy/TiO_2 prepared in the carboxylic acids without hydroxyl group. Furthermore, all the composites could rapidly reach adsorption equilibrium within 30 min and could be reused at least 4 times without losing the adsorption capacity. The adsorption kinetic and thermodynamic data proved that the adsorption process of the employed dyes onto the composites mainly depended on the chemisorption.

1. Introduction

Adsorption is considered as an efficient approach to remove chemical contaminants (*e.g.*, dyes,[1,2] organic acids[3,4] and heavy metal ions[5,6]) from the environment, and the adsorbent is the key factor in the adsorption process. Nowadays, there are various novel adsorbents, such as graphene,[7] metal-organic frameworks,[8] and conducting polymers,[9,10] besides the common activated carbon, used in the environmental field. Among these materials, conducting polymers attract more attention due to the excellent physicochemical properties but generally showed inferior adsorption performance. Many approaches (*e.g.*, formation of composites,[5,11] modification by functional chemicals,[12] doping with counter ions[13]) were employed to improve the adsorption performance of conducting polymers. Composites based on the conducting polymers were commonly used to enhance the adsorption performance by combining the advantages of individual materials. It was reported by Cui *et al.* that polyaniline/attapulgite (PANI/attapulgite) composite displayed the maximum adsorption capacity of over 800 mg L^{-1} for Hg(II),[14] and it was found in our previous work that polypyrrole/TiO_2 (PPy/TiO_2) and PANI/TiO_2 composites showed excellent adsorption performance for organic dyes.[11,15]

It was reported in some literature that the conducting polymers prepared in various acid systems have different adsorption behaviors. Wang *et al.*[9] prepared PANI nanoparticles and 1D nanostructures in protonic acids like HCl, sulfamic acid, citric acid, taurine for the removal of Cr(VI). The results indicated that the PANI prepared in HCl showed the highest adsorption capacity. The investigation on the adsorption behavior of PPy/TiO_2 composites synthesized from HNO_3 or H_2SO_4 solution in our group indicated that the composite prepared from H_2SO_4 solution exhibited a high adsorption capacity of 323 mg g^{-1} for Methylene Blue (MB).[11,16] Moreover, the PANI/TiO_2 composites obtained from mixed acid solution of HNO_3 (0.064 mol L^{-1}) and citric acid (0.1 mol L^{-1}) in our group showed a high adsorption capacity of 454 mg g^{-1} for Acid Red G (ARG).[15] However, the effect of organic acids with various numbers of hydroxyl and carboxylic groups on the adsorption performance of PPy/TiO_2 was rarely investigated so far. Herein, PPy/TiO_2 composites were prepared in diverse carboxylic acids with/without hydroxyl group. The surface physicochemical properties of PPy/TiO_2 composites prepared in different carboxylic acids were

Department of Environmental Science and Engineering, State Key Laboratory of Multiphase Flow in Power Engineering, Xi'an Jiaotong University, Xi'an 710049, P.R. China. E-mail: yanwei@xjtu.edu.cn; jinwen_shi@xjtu.edu.cn

† Electronic supplementary information (ESI) available. See DOI: 10.1039/c6ra06738g

systematically analyzed, and furthermore, the influence of carboxylic acids with/without hydroxyl group on adsorption performance of PPy/TiO_2 composites for ARG and MB was comprehensively discussed.

2. Experimental

2.1. Materials

Acetic acid (AC), succinic acid (SU), tartaric acid (TA) and citric acid (CI) were all purchased from Sinopharm Chemical Reagent Co. Ltd., China, and their molecular structures are displayed in Fig. 1. $FeCl_3 \cdot 6H_2O$, NaOH, HCl, *n*-propanol and tetrabutyl *ortho*-titanate (TBOT, 98%) were of analytical grade and also from Sinopharm Chemical Reagent Co. Ltd, China. Pyrrole monomer (98%) was obtained from Qingquan Pharmaceutical & Chemical Ltd., Zhejiang, China, and was distilled twice under reduced pressure and then stocked in refrigerated bottles with N_2 atmosphere in dark before used. MB (319.86 g mol^{-1}) was purchased from Beijing Chemical Reagent Co. Ltd., China. ARG (509.43 g mol^{-1}) was commercial grade and recrystallized before used in adsorption test. The molecular structures of ARG and MB are shown in Fig. 2. The deionized water used for all experiments was obtained from the EPED-40 TF Superpure Water System, China.

2.2. Synthesis of PPy/TiO_2 composites modified by different carboxylic acids

The synthesis procedure of PPy/TiO_2 composites modified by different carboxylic acids was described as follows. Firstly, a mixture of TBOT and *n*-propanol (volume ratio, 5 : 2) was added into carboxylic acid solution (200 mL, 0.10 mol L^{-1}) with magnetic stirring for 2 h at 65 °C to form a white suspension, which was then cooled to ambient temperature. Afterwards, pyrrole monomer (0.25 mL) was added into the suspension and stirred for 1 h, and then $FeCl_3$ (10 mL, 1.0 mol L^{-1}) solution was added into the suspension dropwise in 1 h accompanied with stirring. After statically aged for 24 h, the resulting mixture was filtrated. The obtained black solid was washed several times with water until the pH value of the eluate became neutral, and then dried at 50 °C for 24 h to get the final products, *i.e.*, the as-prepared PPy/TiO_2 composites named as AC-PPy/TiO_2, SU-PPy/TiO_2, TA-PPy/TiO_2 and CI-PPy/TiO_2 according to the carboxylic acids (AC, SU, TA and CI) used in the synthesis process.

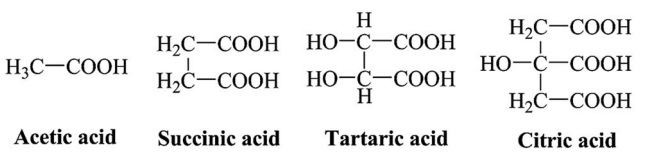

Fig. 1 Molecular structures of acetic, succinic, tartaric and citric acids.

2.3. Characterizations

BET surface area (S_{BET}), total pore volume (V) and average pore radius (R) of PPy/TiO_2 composites were measured at 77 K using Builder SSA-4200 instrument (China). Fourier-transform infrared spectra (FT-IR) were recorded by the KBr pellet method on BRUKER TENSOR 37 (Germany) instrument in the range of 4000–400 cm^{-1}. Thermogravimetric (TG) analyses were performed on Setaram Labsys Evo (France) instrument in N_2 flow at a heating rate of 10 °C min^{-1}.

Zeta potentials were measured with Malvern Zetasizer Nano ZS90 equipment (UK). PPy/TiO_2 composites (5 mg) were added into NaCl solutions (10 mL, 10^{-3} mol L^{-1}) for the measurement. The pH values of NaCl solutions were adjusted from 1 to 13 by diluted HNO_3 (0.1 mol L^{-1}) or NaOH (0.1 mol L^{-1}) solution in order to obtain a series of zeta-potentials of PPy/TiO_2 composites.

2.4. Adsorption experiments

The adsorption experiments of ARG or MB were carried out by shaking the mixture of ARG or MB solution with PPy/TiO_2 composites at 25 °C for a period of time at first. The suspension was then centrifuged at 4000 rpm for 5 min. The obtained supernatant was analyzed by Agilent 8453 UV-Vis spectrophotometer (USA) to evaluate the adsorption capacity of PPy/TiO_2 composites. The absorbance values of ARG and MB solutions were recorded according to the wavelengths of 503 and 665 nm, respectively.

The amounts of dye molecules adsorbed onto PPy/TiO_2 composites Q_t (mg g^{-1}) in a certain time t were calculated from eqn (1):

$$Q_t = \frac{C_0 - C_t}{M} \times V \quad (1)$$

where C_0 (mg L^{-1}) is the initial concentration of dye solution; C_t (mg L^{-1}) is the residual concentration of dye solution at time t (min); V (L) is the solution volume, and M (g) is the mass of PPy/TiO_2 composite.

The adsorption equilibrium of ARG or MB (200, 300 and 500 mg L^{-1}) was evaluated at 25 °C in interval time. A dye concentration of 300 mg L^{-1} was selected to investigate the adsorption kinetics, which were analyzed by using the pseudo-first-order (eqn (2)) and pseudo-second-order models (eqn (3)):

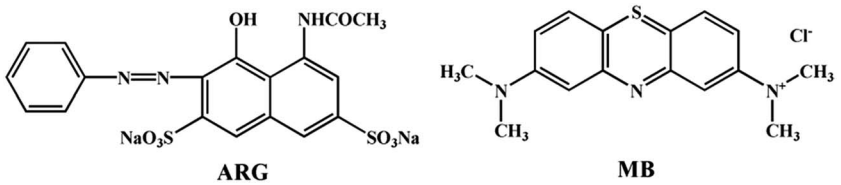

Fig. 2 Molecular structures of ARG and MB.

$$\lg(Q_e - Q_t) = \lg Q_e - \frac{K_1}{2.303} t \quad (2)$$

$$\frac{t}{Q_t} = \frac{1}{K_2 Q_e^2} + \frac{t}{Q_e} \quad (3)$$

where t is the contact time (min); K_1 (min^{-1}) and K_2 (g mg^{-1} $min^{0.5}$) are the rate constants for the pseudo-first-order and pseudo-second-order models, respectively; Q_e (mg g^{-1}) is the adsorption amount at equilibrium state.

Adsorption isotherms of ARG or MB at 25 °C were obtained by mixing different concentrations (50–1200 mg L^{-1}) of ARG or MB solution with PPy/TiO_2 composites (2 g L^{-1}) and then shaking for 120 min in dark, and were analyzed by using the Langmuir (eqn (4)) and Freundlich isotherm models (eqn (5)):

$$Q_t = \frac{Q_{max} K_L C_t}{1 + K_L C_t} \quad (4)$$

$$Q_t = K_F C_t^{1/n} \quad (5)$$

where Q_{max} (mg g^{-1}) is the maximum monolayer molecular adsorption capacity of the adsorbent in Langmuir isotherm model; K_L (L mg^{-1}) and K_F (mg g^{-1}) are the constants of Langmuir and Freundlich isotherm models, respectively. $1/n$ represents the degree of dependence of adsorption on equilibrium concentration in Freundlich isotherm model.

3. Results and discussion

3.1. Characterizations of PPy/TiO_2 composites

The textural characterizations of samples are displayed in Table 1. It could be seen that AC-PPy/TiO_2 and SU-PPy/TiO_2 had larger S_{BET} but smaller average pore radius (R) values, suggesting that the used carboxylic acids with/without hydroxyl group largely impacted the textural properties of PPy/TiO_2 composites. The textural properties would further affect the adsorption performance of PPy/TiO_2 composites.

Table 1 Textural properties of PPy/TiO_2 composites

Composite	S_{BET}/m^2 g^{-1}	V/cm^3 g^{-1}	R/nm
AC-PPy/TiO_2	210.90	0.37	4.11
SU-PPy/TiO_2	221.48	0.20	4.31
TA-PPy/TiO_2	30.37	0.39	21.79
CI-PPy/TiO_2	29.98	0.27	15.59

The FT-IR spectra of samples are shown in Fig. S1† and the assignments are listed in Table 2. All the characteristic peaks of carboxylate,[17,18] O–Ti–O[19] and PPy[20,21] appeared in samples, therefore demonstrating that PPy/TiO_2 composites were successfully formed. Intensities and positions of the bonds related to PPy displayed obvious changes in different composites due to the various carboxylic and hydroxyl groups in the employed acids. It was claimed by Jankovic *et al.* and Weng *et al.* that TiO_2 could form chelate and bridge complexes with hydroxyl and carboxylic groups of organic acids.[22,23] Herein, TiO_2 could exhibit chelate structure with the carboxylic group of acetate acid, bridge structure with the two carboxylic groups of succinic acid, and bridge structure with one hydroxyl group and one carboxylic group of tartaric and citric acids.[24,25] In SU-PPy/TiO_2, TA-PPy/TiO_2 and CI-PPy/TiO_2, hydroxyl and carboxylic groups did not coordinate with TiO_2 completely as evidenced by the obvious characteristic peak of C=O. The existence of hydroxyl or carboxylic group would be favorable to improve the adsorption performance.[25] Furthermore, PPy/TiO_2 composites with stable interface could be formed due to the hydrogen bonding or covalent-like interaction between PPy and the functional groups of modified TiO_2.[26,27]

Fig. 3 shows the TG curves of samples and the relevant data are listed in Table 3. The first stage below 120 °C was generally attributed to the loss of physically adsorbed water.[28] The second stage between 120 and 250 °C is probably due to the loss of structural water and doping ions in PPy.[29,30] TA-PPy/TiO_2 and CI-PPy/TiO_2 showed weight loss larger than that of AC-PPy/TiO_2 and SU-PPy/TiO_2 in this stage, thereby indicating that TA-PPy/TiO_2 and CI-PPy/TiO_2 contained more chemically adsorbed water and doping ions in PPy, and also implying that PPy in both TA-PPy/TiO_2 and CI-PPy/TiO_2 had higher doping level of counter ions. The third stage between 250 and 550 °C was probably assigned to the decomposition of PPy with long molecular backbone.[29] Furthermore, the weight loss for TA-PPy/TiO_2 and CI-PPy/TiO_2 was also higher than that of AC-PPy/TiO_2 and SU-PPy/TiO_2. This result indicated that PPy in TA-PPy/TiO_2 and CI-PPy/TiO_2 had higher polymerization degree, which led to

Table 2 FT-IR absorption bands in PPy/TiO_2 composites and their assignments

Wavenumber/cm^{-1}				
AC-PPy/TiO_2	SU-PPy/TiO_2	TA-PPy/TiO_2	CI-PPy/TiO_2	Assignment
1627	1633	1668	1691	C=O stretching vibration[17,18]
1553	1550	1554	1554	C=C stretching vibration[20,21]
1468	1463	1452	1473	C=N stretching vibration[20,21]
1325	1321	1323	1311	C–H or C–N in-plane deformation mode[20,21]
1192	1182	1193	1193	NH^+ deformation mode[20,21]
1053	1047	1047	1047	C–H or N–H in-plane deformation vibration[20,21]
930	926	926	926	C–H out-of-plane deformation vibration[20,21]
400–1000				O–Ti–O[19]

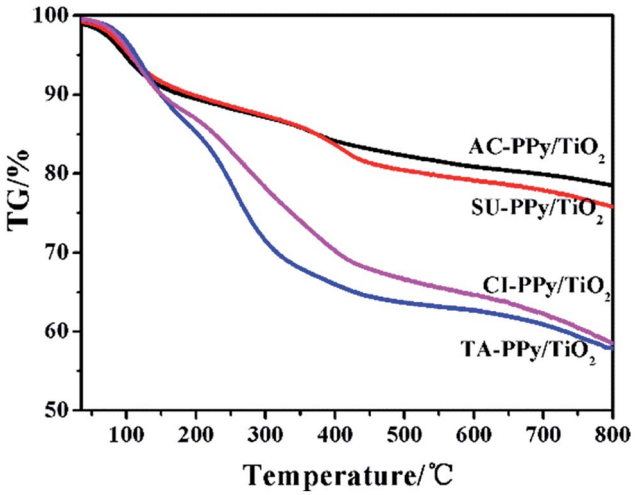

Fig. 3 TG curves of PPy/TiO_2 composites.

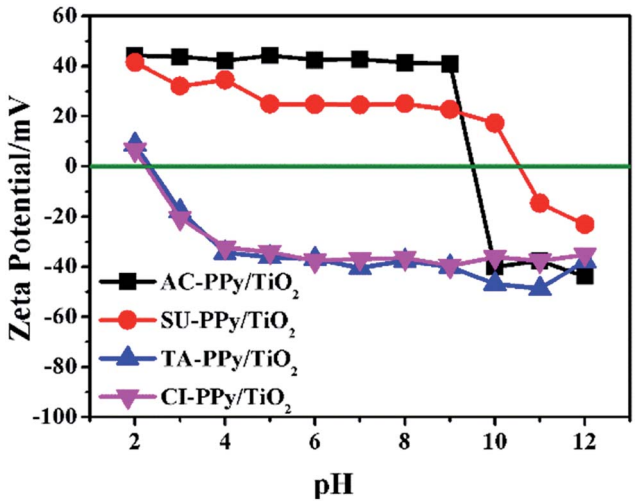

Fig. 4 Zeta potential of PPy/TiO_2 composites.

Table 3 Mass loss of PPy/TiO_2 composites at different stages

	Mass loss/wt%			
Composite	<120 °C	120–250 °C	250–500 °C	>500 °C
AC-PPy/TiO_2	5.69	4.59	5.99	3.78
SU-PPy/TiO_2	5.64	5.03	8.14	4.60
TA-PPy/TiO_2	6.25	10.34	16.32	8.06
CI-PPy/TiO_2	5.46	15.15	15.15	5.75

more PPy in the two composites. The stage in the range of 500–800 °C was mainly due to the decomposition of coordinated carboxylate groups in TiO_2.[25] As suggested by the mass loss data in Table 3, more organic component existed in the PPy/TiO_2 composites prepared in the carboxylic acids with hydroxyl group, and would be beneficial to improve the adsorption performance of PPy/TiO_2 composites.

Fig. 4 presents the zeta potentials of samples. The isoelectric point (pH_{iep}) is the pH value when the zeta potential value is zero. The pH_{iep} values of AC-PPy/TiO_2, SU-PPy/TiO_2, TA-PPy/TiO_2 and CI-PPy/TiO_2 were about 9.49, 10.55, 2.33 and 2.26, respectively, suggesting that the surfaces of AC-PPy/TiO_2, SU-PPy/TiO_2 were positively charged while those of TA-PPy/TiO_2 and CI-PPy/TiO_2 were negatively charged under neutral condition. This phenomenon was similar to that of TiO_2 prepared in various carboxylic acids in our previous work as described as follows.[25] The organic acid with hydroxyl and carboxyl groups could complex with TiO_2, and the TiO_2 prepared in malic and tartaric acids with both hydroxyl and carboxylic groups had low pH_{iep} values due to the free hydroxyl and carboxyl groups on the surface.

3.2. Adsorption experiments

3.2.1. Effect of surface charge of PPy/TiO_2 composites on the adsorption behavior. Fig. 5 presents the adsorption capacities of different dyes onto PPy/TiO_2 composites pretreated by solutions with different pH values adjusted by 0.1 mol L^{-1} of HCl or NaOH solution. Herein, the pretreatment solution with different pH was used to change the charge of PPy/TiO_2 composites. It could be found that the adsorption capacities of AC-PPy/TiO_2, SU-PPy/TiO_2, TA-PPy/TiO_2 and CI-PPy/TiO_2 for different dyes altered when the composites were pretreated by aqueous solution with varied pH values. The adsorption amount of ARG decreased with the increase of pretreatment solution pH from 1 to 13 and the maximum adsorption capacity was achieved at the pH of 1, which suggested that ARG could be easily adsorbed on the acid-treated PPy/TiO_2 composites. Correspondingly, the adsorption amount of MB increased with the increase of pH and reached the largest value at the pH of 13, which indicated that MB could be easily adsorbed on the alkali-treated PPy/TiO_2 composites.

Wang *et al.*[31] announced that the surface of TiO_2 could be either positively or negatively charged in a solution with an appropriate range of pH according to eqn (6) and (7). Moreover, Zhang *et al.*[32] pointed out that PPy exhibited similar phenomenon, *i.e.*, positively charged in acid solution and negatively charged in alkaline solution, which could be represented by eqn (8) and (9) (where X notates the doping ions):

$$Ti\text{–}OH + H^+ \rightarrow Ti\text{–}OH_2^+,\ pH < pH_{iep} \quad (6)$$

$$Ti\text{–}OH + OH^- \rightarrow Ti\text{–}O^- + H_2O,\ pH > pH_{iep} \quad (7)$$

$$PPyX + H^+ \rightarrow PPyXH^+,\ pH < pH_{iep} \quad (8)$$

$$PPyX + OH^- \rightarrow PPyXOH^-,\ pH > pH_{iep} \quad (9)$$

Based on zeta potential analysis, the pH_{iep} values of AC-PPy/TiO_2, SU-PPy/TiO_2, TA-PPy/TiO_2 and CI-PPy/TiO_2 are 9.49, 10.55, 2.33 and 2.26, respectively. It could be further deduced the surfaces of TA-PPy/TiO_2 and CI-PPy/TiO_2 were positively charged when pH was below 3. Correspondingly, TA-PPy/TiO_2 and CI-PPy/TiO_2 could adsorb ARG due to electrostatic interaction, but had relatively poor adsorption capacities for MB owing to electrostatic repulsion. When pH was above 3, TA-PPy/TiO_2 and CI-PPy/TiO_2 composites with negative charges exhibited low ARG adsorption

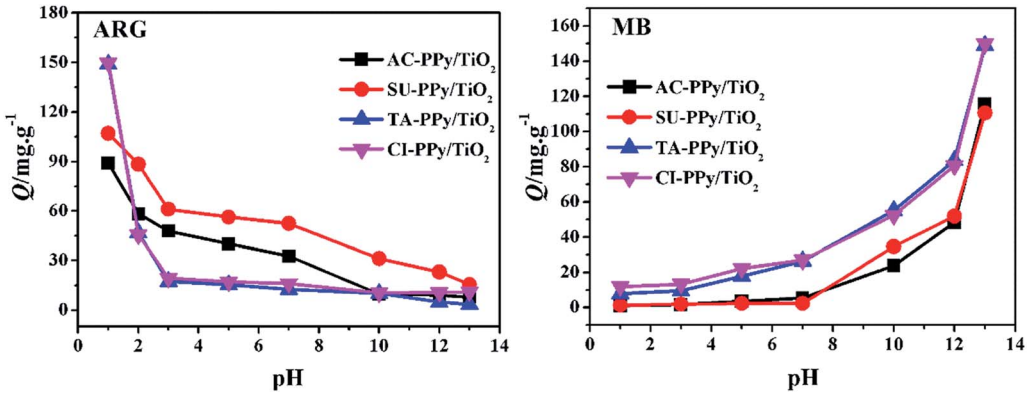

Fig. 5 Effects of pretreatment solution pH on the adsorption capacities of PPy/TiO_2 composites for ARG and MB, respectively.

capacities due to electrostatic repulsion and displayed enhanced MB adsorption ability owing to electrostatic attraction. In contrast, AC-PPy/TiO_2 and SU-PPy/TiO_2 were positively charged when pH was below 10, and were negatively charged when pH was above 10. Accordingly, AC-PPy/TiO_2 and SU-PPy/TiO_2 displayed improved adsorption capacities for MB when pH was over 10. Moreover, TA-PPy/TiO_2 and CI-PPy/TiO_2 possessed more amounts of doping ions and PPy than those in AC-PPy/TiO_2 and SU-PPy/TiO_2 as proved by the TG analysis, and therefore exhibited greater maximum adsorption capacities for both ARG and MB under the optimized pH values for each PPy/TiO_2 composite. Besides, AC-PPy/TiO_2 and SU-PPy/TiO_2 still displayed some adsorption capacities for MB in the pH range of 2–10 although AC-PPy/TiO_2 and SU-PPy/TiO_2 were positively charged under this condition, thus indicating that the interactions between PPy/TiO_2 composites and dyes included not only electrostatic force but also other mechanisms, such as the hydrogen bonding formed between the N–H in PPy and the dyes.[16,33]

According to the above results, in the following experiments, PPy/TiO_2 composites were pretreated with HCl solution (0.1 mol L^{-1}) to adsorb ARG and NaOH solution (0.1 mol L^{-1}) to adsorb MB in order to ensure the best adsorption performance for different dyes.

3.2.2. Adsorption equilibrium and kinetics. It is essential for the adsorbent to remove adsorbate from solution with rapid adsorption kinetic. The influence of contact time on the adsorption of ARG and MB with various initial concentrations is presented in Fig. S2.† It could be observed that the adsorption of dyes proceeded rapidly and experienced three stages. In the first stage (0–10 min), the adsorption was so fast that the adsorption amount sharply increased. The adsorption rate gradually reduced in the second stage (10–30 min), and the adsorption amount increased more and more slowly. After that, the adsorption process reached equilibrium. Accordingly, it was feasible to examine the adsorption process of dyes onto PPy/TiO_2 composites during a period of 120 min in the following experiments.

In addition, with the increase of the initial concentration of dyes, the adsorption amount of ARG or MB onto all PPy/TiO_2 composites increased. However, the adsorption equilibrium time became longer, which could be attributed to the electrostatic repulsion that existed between the adsorbed and free dye molecules hindered the migration of the free dye molecules onto the surface of PPy/TiO_2 composites from the bulk solution.[34] Besides, it could be observed that the adsorption capacities of AC-PPy/TiO_2 and SU-PPy/TiO_2 for ARG were lower than those for MB.

The kinetic curves of PPy/TiO_2 composites are shown in Fig. 6, and the related parameters are calculated and listed in Table 4. It was notable that the pseudo-second-order model

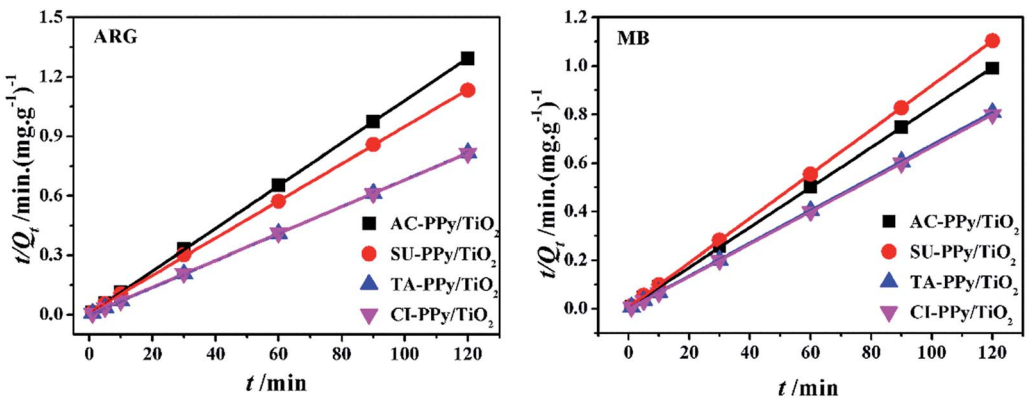

Fig. 6 Pseudo-second-order kinetics plots and fitting lines for ARG and MB adsorbed onto PPy/TiO_2 composites.

Table 4 Parameters of the pseudo-first-order and pseudo-second-order models

		Pseudo-first-order model				Pseudo-second-order model		
Dye	Composite	Q_e[a]/mg g^{-1}	K_1/min^{-1}	Q_e[b]/mg g^{-1}	R^2	K_2/g mg^{-1} min^{-1}	Q_e[b]/mg g^{-1}	R^2
ARG	AC-PPy/TiO$_2$	92.76	0.045	14.27	0.6949	0.024	92.94	0.9999
	SU-PPy/TiO$_2$	105.97	0.043	30.13	0.7945	0.008	106.61	0.9997
	TA-PPy/TiO$_2$	146.96	0.064	15.97	0.7826	0.030	147.27	0.9999
	CI-PPy/TiO$_2$	147.42	0.044	17.93	0.6243	0.016	147.71	0.9999
MB	AC-PPy/TiO$_2$	121.14	0.042	26.37	0.7397	0.011	121.51	0.9999
	SU-PPy/TiO$_2$	108.78	0.081	38.02	0.9437	0.011	109.53	0.9999
	TA-PPy/TiO$_2$	148.51	0.069	10.03	0.6371	0.054	148.59	1.0000
	CI-PPy/TiO$_2$	149.98	0.073	0.75	0.3937	0.180	149.92	1.0000

[a] Q_e is obtained from the experimental data. [b] Q_e was calculated from the kinetics model.

(Fig. 6) was more appropriate than the pseudo-first-order model (Fig. S3†) to describe the adsorption behavior of the selected dyes onto PPy/TiO$_2$ composites, because based on the pseudo-second-order model, the correlation coefficients (R^2 = 0.9997–1.0) were closer to 1, and the calculated values of Q_e were almost equal to the experimental values. It was thus demonstrated that the adsorption of dyes onto PPy/TiO$_2$ composites was mainly ascribed to chemisorption.[35,36]

3.2.3. Adsorption isotherm. The adsorption isotherm at 25 °C was investigated to describe the interaction between dyes and PPy/TiO$_2$ composites. The experimental data (dots), Langmuir (solid line) and Freundlich (dotted line) adsorption isotherm fitting curves for ARG and MB are represented in Fig. 7. The corresponding fitting data are listed in Table 5. It could be deduced based on the fitting curves and correlation coefficients (R^2) that Langmuir model was more reasonable to describe the adsorption process of the dyes onto PPy/TiO$_2$ composites, thus suggesting that only monolayer adsorption happened and hence limited the adsorption sites of PPy/TiO$_2$ composites. The maximum adsorption capacity (Q_{max}) followed an order of CI-PPy/TiO$_2$ > TA-PPy/TiO$_2$ > SU-PPy/TiO$_2$ > AC-PPy/TiO$_2$ for both ARG and MB, which indicated that the carboxylic acid with hydroxyl group was beneficial to improve the adsorption performance of PPy/TiO$_2$ composites. The values of $1/n$ for Freundlich model were located in the range of 0.1–0.5, indicating that the adsorption processes could be easily initiated. Furthermore, the comparison of the adsorption performance of different adsorbents for MB is shown in Table 6. It was indicated that the adsorption performance of PPy/TiO$_2$ composites prepared in carboxylic acid with hydroxyl group were better than that of other adsorbents listed therein. The PPy/TiO$_2$ composites prepared in carboxylic acid with hydroxyl group, *i.e.*, CI-PPy/TiO$_2$ and TA-PPy/TiO$_2$, showed not only higher adsorption capacity, but also shorter equilibrium time.

3.2.4. Regeneration. In view of the effect of surface charges on the adsorption capacity of PPy/TiO$_2$ composites, it could be deduced that ARG and MB could be desorbed from PPy/TiO$_2$ composites by the corresponding treatment of alkaline and acid, respectively. Thus, 0.1 mol L^{-1} of NaOH and HCl were employed as desorption agent for ARG and MB, respectively. The desorbed PPy/TiO$_2$ composite was used to adsorb dye solution (300 mg L^{-1}) again. The regeneration results are displayed in Fig. 8. It was observed that the adsorption capacity of all composites for ARG and MB showed little reduction after adsorption–desorption for 4 cycles, therefore suggesting that PPy/TiO$_2$ composites had excellent regeneration performance. The photographs of CI-PPy/TiO$_2$ composite adsorbed ARG and MB for 4 cycles are shown in Fig. 9.

3.2.5. Thermodynamics. The thermodynamic parameters, such as change of standard Gibbs free energy ΔG^0 (kJ mol^{-1}), entropy ΔS^0 (J (mol^{-1} K^{-1})) and enthalpy ΔH^0 (kJ mol^{-1}) for the

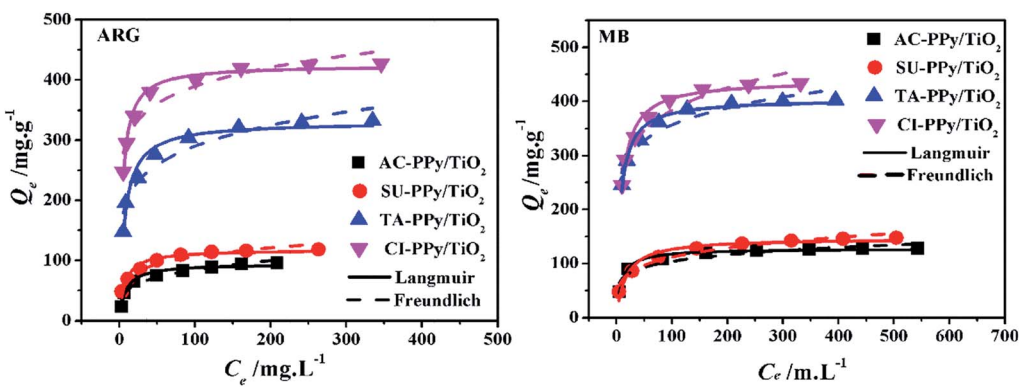

Fig. 7 Langmuir and Freundlich adsorption isotherm models of ARG and MB onto the as-prepared composites.

Table 5 Parameters of Langmuir and Freundlich adsorption isotherm models

		Langmuir model			Freundlich model		
Dye	Composite	Q_{max}/mg g^{-1}	K_L/L mg^{-1}	R^2	K_F/mg g^{-1}	$1/n$	R^2
ARG	AC-PPy/TiO_2	94.74	0.13	0.9712	28.67	0.24	0.9342
	SU-PPy/TiO_2	118.17	0.14	0.9471	45.26	0.18	0.9309
	TA-PPy/TiO_2	330.76	0.14	0.9669	136.80	0.16	0.9170
	CI-PPy/TiO_2	424.75	0.21	0.9684	232.36	0.11	0.8992
MB	AC-PPy/TiO_2	127.78	0.11	0.9831	49.83	0.16	0.8835
	SU-PPy/TiO_2	147.09	0.061	0.9411	43.13	0.21	0.9553
	TA-PPy/TiO_2	404.31	0.14	0.9687	203.74	0.12	0.9177
	CI-PPy/TiO_2	439.61	0.12	0.9777	195.85	0.15	0.9221

Table 6 Comparison of the adsorption performance of different adsorbents for MB

Adsorbent	Q_{max}/ mg g^{-1}	Equilibrium time/h	Reference
TA-PPy/TiO_2	404.31	0.5	This work
CI-PPy/TiO_2	439.61	0.5	This work
Bamboo-based activated carbon	454	48	37
Activated carbon	270	>400	38
Rattan sawdust-activated carbon	294.12	24	39
Activated carbon from oil palm wood	90.9	—	40
Polyacrylonitrile fiber treated with hyperbranched polyethylenimine	161	1.0	41
2D MoS_2 nanosheets	146.43	1.0	42

adsorption of ARG and MB by CI-PPy/TiO_2 composite are determined by eqn (10) and (11):

$$\ln K_L = \frac{\Delta S^0}{R} + \frac{-\Delta H^0}{RT} \quad (10)$$

$$\Delta G^0 = -RT \ln K_L \quad (11)$$

where K_L is the constant of Langmuir model, R (8.314 J (mol^{-1} K^{-1})) is the gas constant and T (K) is kelvin temperature used in the adsorption process.

CI-PPy/TiO_2 composite had the best adsorption ability for both ARG and MB as discussed above, and hence was selected as the representative composite to investigate the adsorption thermodynamics of PPy/TiO_2 composites. The relationship between the Q_e value of ARG and MB onto CI-PPy/TiO_2 and the initial concentration at different Kelvin temperatures (288, 298, 308 and 318 K) are displayed in Fig. S4.† Meanwhile, the fitting curves of T^{-1} *vs.* ln K_L for ARG and MB are shown in Fig. 10, and the relevant parameters calculated from the fitting curves were listed in Table 7. It was observed that the equilibrium adsorption capacity for both ARG and MB onto CI-PPy/TiO_2 increased with the temperature, which suggested that the higher temperature was favorable for the adsorption.[43,44]

The positive values of ΔH^0 proved that the process was endothermic in nature.[45] Furthermore, the values of ΔH^0 for

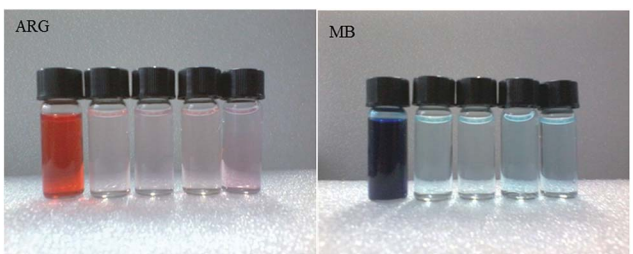

Fig. 9 Photographs of CI-PPy/TiO_2 adsorbed ARG and MB for 4 cycles.

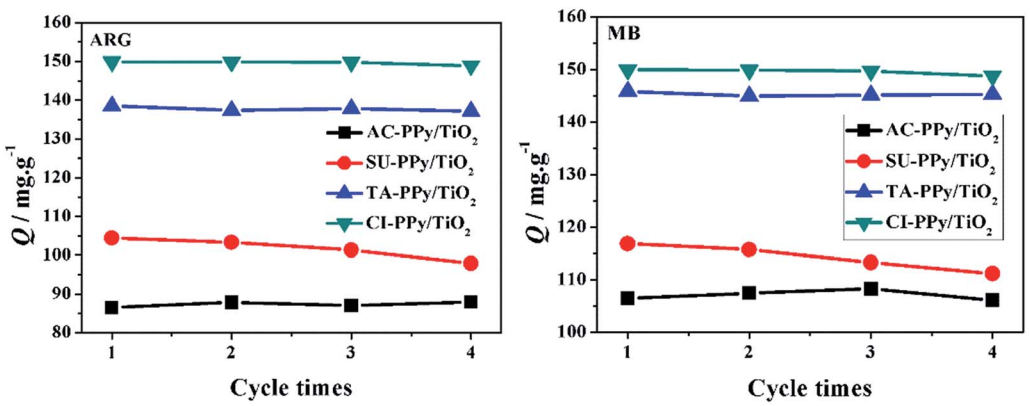

Fig. 8 Regeneration performances of PPy/TiO_2 composites.

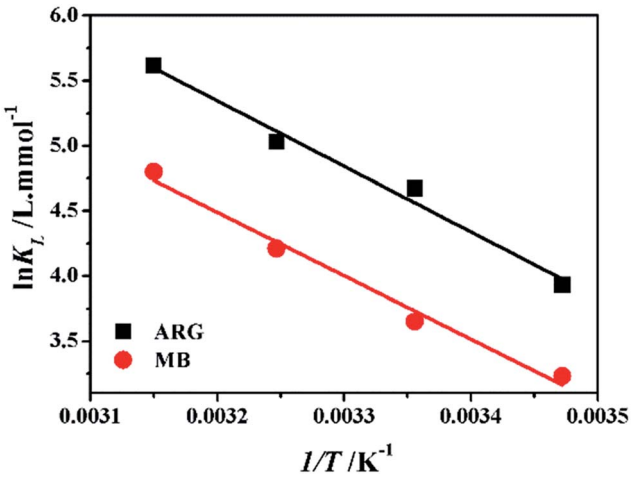

Fig. 10 Linear dependence of T^{-1} on ln K_L for ARG and MB adsorbed onto CI-PPy/TiO_2.

Table 7 Thermodynamic and Langmuir parameters for ARG and MB adsorbed onto CI-PPy/TiO_2 at different temperatures

Dye	Temperature/ K	Q_{max}/ mg g^{-1}	K_L/ L mg^{-1}	ΔG^0/ kJ mol^{-1}	ΔS^0/ J mol^{-1} K^{-1}	ΔH^0/ kJ mol^{-1}
ARG	288	414.10	50.94	−9.52	178.47	41.88
	298	424.75	106.98	−11.30		
	308	437.98	152.83	−13.09		
	318	447.22	275.09	−14.87		
MB	288	431.57	25.27	−7.57	167.09	40.55
	298	439.61	38.38	−9.24		
	308	449.20	67.17	−10.91		
	318	458.84	121.55	−12.58		

both ARG and MB were over 40 kJ mol^{-1}, thus indicating that chemisorption was dominant in the adsorption process,[46,47] which was consistent with the adsorption kinetic result. The positive values of ΔS^0 indicated the increase in disorder in the adsorption system. The negative values and decline trend of ΔG^0 with the increase of temperature demonstrated that the adsorption process was spontaneous.

3.3. Adsorption mechanism

It is generally accepted that higher specific surface area is contributed to the great adsorption capacity of an adsorbent.[8,48] However, it was notable that the adsorption capacities of PPy/TiO_2 composites for both ARG and MB were inversely proportional to S_{BET}. Specifically, CI-PPy/TiO_2 and TA-PPy/TiO_2 with smaller S_{BET} displayed higher adsorption capacity for both ARG and MB, whereas AC-PPy/TiO_2 and SU-PPy/TiO_2 with the larger S_{BET} exhibited lower adsorption capacity. This result implied that the specific surface area was not a key factor for the adsorption behavior of PPy/TiO_2 composites, which is similar to the reported results by our group.[11,16]

In contrast, surface charge of PPy/TiO_2 composites played an important role in the adsorption as discussed in Part 3.2.1. The adsorption capacity of PPy/TiO_2 composites varied with the surface charge. When the pH values of pretreatment solutions were below the pH_{iep}, PPy/TiO_2 composites carried positive charge, and thus could adsorb anionic dye ARG mainly by virtue of electrostatic attraction. Conversely, when the pH values of pretreatment solutions were over the pH_{iep}, PPy/TiO_2 composites would be negatively charged, which inhibited the adsorption behavior due to the effect of electrostatic repulsion. The opposite phenomenon appeared in the adsorption process of MB onto PPy/TiO_2 composites. The above results demonstrated that electrostatic interaction was the main adsorption force. Furthermore, as discussed in Part 3.2.1., PPy/TiO_2 composites still had adsorption ability (despite of the lower removal efficiency) for ARG and MB no matter that the pH value was above or below the pH_{iep}, indicating that other interactions existed between dyes and PPy/TiO_2 composites. It was claimed by Yang *et al.* and our group that hydrogen bonding was another interaction between dyes and the related adsorbents besides electrostatic force.[11,49] It was reasonable to deduce that the interactions between PPy/TiO_2 composites and dyes in the adsorption process were mainly electrostatic interaction and hydrogen bonding, and the electrostatic interaction played the major role. This deduction was consistent with not only the kinetic and thermodynamic results in this study but also other previous reports.[33,34]

4. Conclusion

PPy/TiO_2 composites prepared in acetate, succinic, tartaric and citric acids were employed to adsorb anionic dye ARG and cationic dye MB. The surface physicochemical properties of as-prepared composites were very different from each other due to use of varied carboxylic acids with/without hydroxyl group, and these differences further impacted the adsorption capacity of the as-prepared composites. Positive surface charge was favorable for the adsorption of anionic dye ARG onto the PPy/TiO_2 composites, whereas negative surface charge was beneficial for the adsorption of cationic dye MB. All the composites could remove the selected dyes from aqueous solutions rapidly with adsorption equilibrium time no more than 30 min. TA-PPy/TiO_2 and CI-PPy/TiO_2 modified by carboxylic acids with hydroxyl group exhibited higher adsorption capacity than those of PPy/TiO_2 composites prepared in carboxylic acids without hydroxyl group. CI-PPy/TiO_2 displayed the highest adsorption capacity for both ARG (424.75 mg L^{-1}) and MB (439.61 mg L^{-1}) at 25 °C. Besides, the adsorption capacity of all PPy/TiO_2 composites showed almost no loss after adsorption–desorption at least 4 cycles. The adsorption process of the selected dyes onto the composites was an endothermic spontaneous process. The adsorption mechanism was mainly electrostatic interaction and hydrogen bonding. In a word, the preparation within different carboxylic acids with/without hydroxyl group obviously affected the surface physicochemical properties of PPy/TiO_2 composites, and further impacted their adsorption abilities.

Acknowledgements

The authors gratefully acknowledge the financial supports from the National Natural Science Foundation of China (Grant No.

21307098), and the Shaanxi Science and Technology Coordination Innovation Project, China (2015KTZDSF01-02).

References

1 G. Crini and P.-M. Badot, *Prog. Polym. Sci.*, 2008, **33**, 399–447.
2 T. Yao, S. Guo, C. Zeng, C. Wang and L. Zhang, *J. Hazard. Mater.*, 2015, **292**, 90–97.
3 X. Ling, H. B. Li, H. W. Zha, C. L. He and J. H. Huang, *Chem. Eng. J.*, 2016, **286**, 400–407.
4 C. Jung, N. Phal, J. Oh, K. H. Chu, M. Jang and Y. Yoon, *J. Hazard. Mater.*, 2015, **300**, 808–814.
5 V. Chandra and K. S. Kim, *Chem. Commun.*, 2011, **47**, 3942–3944.
6 C. Y. Cao, J. Qu, W. S. Yan, J. F. Zhu, Z. Y. Wu and W. G. Song, *Langmuir*, 2012, **28**, 4573–4579.
7 Y. Shen, Q. L. Fang and B. L. Chen, *Environ. Sci. Technol.*, 2015, **49**, 67–84.
8 J. R. Li, R. J. Kuppler and H. C. Zhou, *Chem. Soc. Rev.*, 2009, **38**, 1477–1504.
9 J. Wang, K. K. Zhang and L. Zhao, *Chem. Eng. J.*, 2014, **239**, 123–131.
10 M. Bhaumik, R. McCrindle and A. Maity, *Chem. Eng. J.*, 2013, **228**, 506–515.
11 J. J. Li, J. T. Feng and W. Yan, *Appl. Surf. Sci.*, 2013, **279**, 400–408.
12 Z. H. Zhang, Y. Liang, P. Liang, C. Li and S. M. Fang, *Polym. Int.*, 2011, **60**, 703–710.
13 D. Mahanta, G. Madras, S. Radhakrishnan and S. Patil, *J. Phys. Chem. B*, 2009, **113**, 2293–2299.
14 H. Cui, Y. Qian, Q. Li, Q. Zhang and J. P. Zhai, *Chem. Eng. J.*, 2012, **211**, 216–223.
15 N. Wang, J. J. Li, W. Lv, J. T. Feng and W. Yan, *RSC Adv.*, 2015, **5**, 21132–21141.
16 J. J. Li, Q. Zhang, J. T. Feng and W. Yan, *Chem. Eng. J.*, 2013, **225**, 766–775.
17 F. Granato, A. Bianco, C. Bertarelli and G. Zerbi, *Macromol. Rapid Commun.*, 2009, **30**, 453–458.
18 J. Wang, K. Zhang, L. Zhao, W. Ma and T. Liu, *Synth. Met.*, 2014, **188**, 6–12.
19 N. T. Nolan, M. K. Seery and S. C. Pillai, *J. Phys. Chem. C*, 2009, **113**, 16151–16157.
20 J. Wang and X. Y. Ni, *Solid State Commun.*, 2008, **146**, 239–244.
21 N. V. Blinova, J. Stejskal, M. Trchova, J. Prokes and M. Omastova, *Eur. Polym. J.*, 2007, **43**, 2331–2341.
22 I. A. Jankovic, Z. V. Saponjic, M. I. Comor and J. M. Nedeljlkovic, *J. Phys. Chem. C*, 2009, **113**, 12645–12652.
23 Y. X. Weng, L. Li, Y. Liu, L. Wang and G. Z. Yang, *J. Phys. Chem. B*, 2003, **107**, 4356–4363.
24 M. T. Nguyen-Le and B. K. Lee, *Chem. Eng. J.*, 2015, **281**, 20–33.
25 J. T. Feng, J. W. Zhu, W. Lv, J. J. Li and W. Yan, *Chem. Eng. J.*, 2015, **269**, 316–322.
26 X. Li, G. Jiang, G. He, W. Zheng, Y. Tan and W. Xiao, *Chem. Eng. J.*, 2014, **236**, 480–489.
27 Q. Cheng, Y. He, V. Pavlinek, C. Li and P. Saha, *Synth. Met.*, 2008, **158**, 953–957.
28 C. Lai, G. R. Li, Y. Y. Dou and X. P. Gao, *Electrochim. Acta*, 2010, **55**, 4567–4572.
29 M. Wei and Y. Lu, *Synth. Met.*, 2009, **159**, 1061–1066.
30 T. Sugimoto and X. P. Zhou, *J. Colloid Interface Sci.*, 2002, **252**, 347–353.
31 W.-Y. Wang and Y. Ku, *Colloids Surf., A*, 2007, **302**, 261–268.
32 X. Zhang and R. B. Bai, *Langmuir*, 2003, **19**, 10703–10709.
33 X. Zhang, R. B. Bai and Y. W. Tong, *Sep. Purif. Technol.*, 2006, **52**, 161–169.
34 X. Zhang and R. B. Bai, *J. Mater. Chem.*, 2002, **12**, 2733–2739.
35 Y. S. Ho and G. McKay, *Process Saf. Environ. Prot.*, 1998, **76**, 332–340.
36 G. Darmograi, B. Prelot, G. Layrac, D. Tichit, G. Martin-Gassin, F. Salles and J. Zajac, *J. Phys. Chem. C*, 2015, **119**, 23388–23397.
37 B. H. Hameed, A. T. M. Din and A. L. Ahmad, *J. Hazard. Mater.*, 2007, **141**, 819–825.
38 S. B. Wang and Z. H. Zhu, *Dyes Pigm.*, 2007, **75**, 306–314.
39 B. H. Hameed, A. L. Ahmad and K. N. A. Latiff, *Dyes Pigm.*, 2007, **75**, 143–149.
40 A. L. Ahmad, M. M. Loh and J. A. Aziz, *Dyes Pigm.*, 2007, **75**, 263–272.
41 Y. Fan, H. J. Liu, Y. Zhang and Y. Chen, *J. Hazard. Mater.*, 2015, **283**, 321–328.
42 X. Q. Qiao, F. C. Hu, F. Y. Tian, D. F. Hou and D. S. Li, *RSC Adv.*, 2016, **6**, 11631–11636.
43 S. B. Wang, Y. Boyjoo, A. Choueib and Z. H. Zhu, *Water Res.*, 2005, **39**, 129–138.
44 Y. S. Al-Degs, M. I. El-Barghouthi, A. H. El-Sheikh and G. M. Walker, *Dyes Pigm.*, 2008, **77**, 16–23.
45 G. Zhao, J. Li, X. Ren, C. Chen and X. Wang, *Environ. Sci. Technol.*, 2011, **45**, 10454–10462.
46 M. Kara, H. Yuzer, E. Sabah and M. S. Celik, *Water Res.*, 2003, **37**, 224–232.
47 C.-H. Wu, *J. Hazard. Mater.*, 2007, **144**, 93–100.
48 Y. S. Li and J. L. Shi, *Adv. Mater.*, 2014, **26**, 3176–3205.
49 D. Yang and B. R. Mattes, *Synth. Met.*, 2008, **158**, 654–660.

